scientific reports

Check for updates

OPEN

Simulation and experimental research on drilling and rock breaking mechanisms of anchor drill rigs with analysis of drilling feedback signals

Xiao-He Wang, Zhi-Qiang Zhao✉ & Wu Jing

In order to alleviate the problem of tense mining succession in coal mines, this study starts from the perspective of rapid roadway excavation roadway support efficiency, and researches on the mechanism of anchored drilling drilling for drilling and rock breaking, establishes the functional relationship equation between the drilling bit cutting rock-breaking force and the energy required to break the unit volume of rock, and verifies the drilling through numerical simulation, self-research drilling experiments on different lithologies and parameters of drilling with drilling, and collects the feedback parameters of displacement, rotational speed, thrust, and torque drilling against theThe feedback parameters of displacement, rotational speed, thrust and torque drilling were collected and analyzed. The research results show that the average speed of drilling, the rotational speed of the drill bit and the rock strength have a negative correlation trend, and the thrust and torque have a positive correlation trend with the rock strength, and the feedback signal of drilling can realize the judgment of the rock strength, realize the prediction of the structure of the surrounding rock, and improve the efficiency of the roadway support in the roadway of rapid excavation roadway support.

Keywords Mining succession tension, Rapid tunneling, Drilling breakthrough mechanisms, Self-developed drilling experiments, Drilling feedback signals

With the large-scale promotion of mine intelligence and mechanization, the problem of tense succession of coal mining is becoming more and more prominent[1,2]. The traditional unified support is difficult to meet the rapid requirements of the roadway, and the support efficiency has become one of the important influencing factors restricting the rapid roadway excavation. Anchor hole drilling is a necessary operation process for tunnel boring, if the feedback signal of anchor hole drilling process can be used to detect the peripheral rock structure of the tunnel, make decisions on tunnel support, and realize tunnel zoning support, it can not only greatly improve the efficiency of tunnel support, but also greatly reduce the occurrence of the accident of the roof plate of the tunnel. Therefore, the research on the mechanism of drilling rock breakage and drilling feedback signal change in the drilling process of anchoring holes is one of the key technologies to realize the rapid tunneling of the roadway, and also one of the important means to alleviate the tightness of the mining succession[3,4].

Many scholars have researched the mechanism of rock-breaking by drilling in the drilling process. As early as 1881, H.R. Hertz studied the elastomer contact theory and carried out the experiment of applying stress to rock to make it broken, which opened the door for many scholars at home and abroad to study the rock-breaking theory in depth, and the more classical models are Evans, Nishimatsu and The more classical models are Evans, Nishimatsu and Dongmin who proposed the maximum tensile stress theory, shear stress theory and fracture mechanics respectively. Numerous researchers have continued to study and explore on the basis of classical models in order to be able to more accurately describe and predict the process of rock breaking by drilling[5–12].

Cheng et al.[13] conducted a series of cutting tests on three kinds of rocks at different cutting depths, backward inclination angles and cutting speeds, and used a high-speed video camera to record the formation process of rock chips frame by frame, which revealed the mechanism of rock-breaking by drilling. Wang et al.[14] established a mathematical model of rock breaking strength and verified the relationship between rock breaking strength

School of Energy and Mining Engineering, China University of Mining and Technology (Beijing), Beijing 100083, China. ✉email: 809762151@qq.com

and cutting speed, cutting depth, rock lithology and wellbore shape through experiments and numerical simulations. Liu, Zhu et al.[15] established a model of rotary impact cutting rock by drill bit through finite element software, and found that brittle damage usually occurs in hard rock when it is subjected to rotary impact cutting by the drill bit. Saksala[16] utilized the finite element simulation means to study the dynamic interaction process between the drill bit and rock, and established a finite element model of the interaction between the percussion drilling well and the hard rock. The finite element model of interaction was established to simulate the dynamic interaction between drill bit and rock, and the effects of different influencing factors on rock fragmentation and drilling were analyzed. Zhu Xiaohua, Liu Weiji et al.[17] established a numerical simulation model of rock specimen composed of particle clusters using PFC particle flow software, and investigated the influencing factors of the rock damage form. The results show that the rock shows plastic damage when the cutting depth is shallow, while the rock shows brittle damage when the cutting depth reaches a certain value.

Based on the mechanisms of drilling and rock fragmentation, numerous researchers have examined the correlation between drilling feedback signals and the structural characteristics of surrounding rock formations. This body of work provides a significant theoretical framework for the real-time detection of surrounding rock structures during drilling operations. Zhang[18] investigated the drilling dynamics of typical coal mine tunnel anchor holes, revealing that drilling vibration signals can rapidly and effectively discern the characteristics of typical coal-bearing strata, yielding favorable recognition results. Liu[19] employed finite element analysis to simulate the drilling processes of various rock types under differing stress conditions, analyzing the drilling results in coal tunnel roofs. Their findings indicate that the average Rate of Penetration can serve as a reliable indicator for differentiating between various rock types. Fu[20,21] addressing the complexities and variability of rock layer structures in coal tunnel roofs, as well as the challenges associated with detecting deteriorated areas, explored the relationship between rock hardness and the drilling characteristics of drill bits. They also examined the vibration characteristics of the drill rod under varying drilling power conditions through theoretical analysis and simulations conducted using ABAQUS finite element software. Han[22] proposed a method for in-situ vibration measurement of mine drills and developed a drill vibration measurement system, which was tested in both laboratory and field settings. Niu[23] designed and constructed a drilling experimental platform, conducted laboratory experiments, and elucidated the response characteristics of the drill rig during the drilling and rock-breaking processes.

Liu[24] equipped a pneumatic impact rotary drill with a digital monitoring system and conducted field drilling experiments, during which they collected real-time drilling parameters. The findings suggest that variations in these real-time drilling parameters during the rock drilling process can effectively reflect changes in rock strength. Wang[25], utilizing drilling parameters obtained from four micro-drilling experiments, employed fitting regression analysis and machine learning regression techniques to predict the uniaxial compressive strength of rocks. Their work offers novel methodologies for the real-time in-situ measurement of rock strength and the recognition of strata drillability. Wang[26] performed drilling experiments aimed at rapidly characterizing rock mechanical properties by modifying thrust conditions to investigate the relationship between rock uniaxial compressive strength and drilling parameters. Wang[27] advocated for the application of digital drilling technology to assess rock uniaxial compressive strength and conducted digital drilling experiments on rocks of varying strengths, demonstrating a quantitative relationship between rock uniaxial compressive strength and real-time drilling parameters.

Rodgers et al.[28] established the rotation speed and Rate of Penetration parameters of the drill rig in their experiments, concurrently recording the torque and thrust signals obtained during the drilling of four rock types with varying strengths. Their analysis revealed a significant correlation between the torque-to-drilling-speed ratio and the specific energy associated with the drilling process. Yaşar et al.[29] examined the relationship between real-time drilling parameters and rock properties, discovering that Rate of Penetration exhibited a negative correlation with both drilling depth and time. Furthermore, they demonstrated that the uniaxial compressive strength of rocks could be expressed in terms of the specific energy of drilling, thereby offering new insights for real-time rock type identification. Shreedharan et al.[30] investigated real-time rock type identification and found that by analyzing and processing the acoustic signals generated during drilling, they could effectively distinguish between different rock types. Kumar et al.[31,32] revealed that sound signals captured by sensors, following noise reduction and Fourier transformation, could indicate variations in the uniaxial compressive and tensile strengths of rocks. Vardhan[33,34], utilizing a custom-built real-time rock type identification device in a laboratory setting, explored the relationship between real-time drilling parameters and rock strength. He identified a strong correlation between the sound pressure level within the drilling parameters and the compressive strength of the rocks, concluding that the uniaxial compressive strength could be predicted based on the sound pressure level. Hoffman[35], leveraging insights from the smart drilling project and the expansion of the parvnet control model, developed a computer monitoring technology for a mast-type model roof drill. Itakura et al.[36–39] conducted experimental studies on pneumatic anchor drills equipped with a data recording system. This system, by monitoring torque, thrust, and other drilling parameters, facilitates geological structure inference and the optimization of support schemes.

The theory of drilling to break rock emphasizes that during the drilling process, the drill bit is subjected to the action of the rock mass will produce a series of feedback signals, which are closely related to the physical and mechanical properties of the rock body.Therefore, an accurate grasp of these rules of change not only helps to quickly and accurately understand the characteristics of the underground peripheral rock, provides a key basis for real-time decision-making on the support program, effectively improves the support efficiency, but also provides a key technology for the development of rapid tunneling. This paper From Drill Bits Drilling and breaking rock Mechanisms Research. To analyze the relationship between the cutting force of the drill bit cutting to break rock and the amount of rock per unit volume broken energy required Energy relationship The numerical simulation is used to analyze the relationship between the drilling feedback signals of the drill

bit under different drilling conditions. the feedback signals of the drill bit under different drilling conditions, using numerical simulation to analyze the relationship. Self study Develop develop a set of drilling experimental platforms capable of collecting drilling parameters in real time, and to the Three different prefabricated rocks conducted drilling experiments, the test results, numerical simulation results and theoretical calculations were cross-checked to determine the accuracy of the study.

Analysis of drilling and rock-breaking mechanisms

During drilling operations, the mechanisms of drilling and rock fragmentation are predominantly facilitated by the application of thrust in the vertical direction by the drill rod, which advances the drill bit, in conjunction with torque in the horizontal direction that enables the rotation of the drill bit. To investigate the mechanisms of drilling and rock fragmentation, calculations were conducted to assess the cutting forces exerted by polycrystalline diamond compact (PDC) drill bit on the rock, as well as the mechanical specific energy during the drilling process. These calculations were based on established methodologies for determining cutting forces and analyzing cutting energy.

In Fig. 1, during the drilling process, the rock being penetrated by the drill bit is predominantly subjected to axial thrust F_n and horizontal force F_t. The adjacent rock block primarily experiences pure shear failure, while the resultant force F signifies the cutting force acting on the rock, with a cutting depth denoted as (h).

Based on the diagram, it is assumed that PDC drill bit penetrates the rock object OAB. The cutting force is distributed along the segment OA, with stress concentration initially occurring at point O and gradually diminishing along OA. Therefore, if the cutting force along the OA segment adheres to a power function distribution, it can be mathematically represented as:

$$F_a = a(L - x)^b \tag{1}$$

where F_a represents the cutting force distribution function along the OA segment; L represents the distance between O and A, $L = \frac{h}{\sin\alpha}$; h represents the cutting depth of the drill bit; a is the unknown constant coefficient; x represents the distance from a point on OA to O; and b represents the coefficient of the function distribution; α represents the angle along OA in the cutting direction; β represents the inclination angle of the composite blade of the drill bit; and γ represents the angle between F and the normal to the composite blade.

Based on the preceding assumption, the resultant force F' acting on the cut rock body along the segment OA, attributable to the power function distribution of the cutting force, is expressed as follows:

$$F' = \int_0^L F_a dx \tag{2}$$

According to the principles of static equilibrium, F and F' along the segment OA must sum to zero:

$$F + F' = 0 \tag{3}$$

$$F = -\int_0^{\frac{h}{\sin\alpha}} a(\frac{h}{\sin\alpha} - x)^b dx \tag{4}$$

The integration of Eq. (4) facilitates the calculation of the coefficient, as follows:

$$a = -F\,(b+1)\,(\frac{\sin\alpha}{h})^{b+1} \tag{5}$$

The distribution of the cutting force along segment OA at point F_a has been determined:

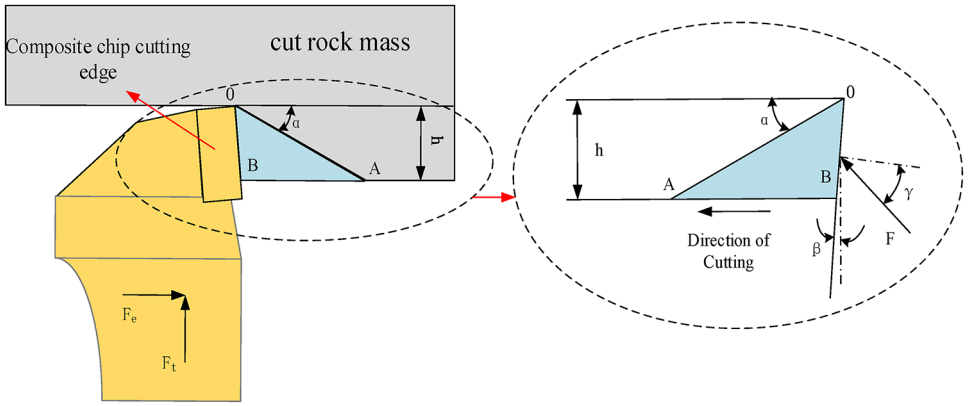

Fig. 1. Schematic of rock stress distribution during drilling process.

$$F_a = -F\,(b+1)\,(\frac{\sin\alpha}{h})^{b+1}(\frac{h}{\sin\alpha}-x)^b \tag{6}$$

During cutting, stress concentration occurs at point O, therefore the cutting force is greatest at point O, and the rock first breaks at point O, which is the $x=0$ position. Substituting this into Eq. (6) yields:

$$F_a = -F\,(b+1)\,\frac{\sin\alpha}{h} \tag{7}$$

The decomposition of vector F_a along the tangential and normal directions of segment OA allows for the calculation of shear stress and normal stress at point O:

$$\begin{cases} \tau_O = -F\,(b+1)\,\frac{\sin\alpha}{h}\cos(\alpha+\beta+\gamma) \\ \sigma_O = -F\,(b+1)\,\frac{\sin\alpha}{h}\sin(\alpha+\beta+\gamma) \end{cases} \tag{8}$$

where γ represents the angle between F and the normal to the composite blade.

Since point O is the initial point of failure, it is posited that the failure at this location is characterized as pure shear failure, consistent with Mohr-Coulomb strength criterion. Based on Mohr-Coulomb criterion, the following derivation can be made:

$$\tau = c + \sigma\tan\varphi \tag{9}$$

where, τ represents the shear stress on the shear plane; β represents the normal stress on the shear plane; c represents the cohesion of the rock; and φ represents the internal friction angle of the rock.

By substituting Eq. (8) into Eq. (9), one can derive the following results:

$$-F\,(b+1)\,\frac{\sin\alpha}{h}\cos(\alpha+\beta+\gamma) = c - F\,(b+1)\,\frac{\sin\alpha}{h}\sin(\alpha+\beta+\gamma)\tan\varphi \tag{10}$$

The solution can be obtained as follows:

$$F = \frac{ch}{(b+1)\sin\alpha\,[\sin(\alpha+\beta+\gamma)\tan\varphi - \cos(\alpha+\beta+\gamma)]} \tag{11}$$

According to the principle of minimum energy consumption, the direction of damage at point O should align with the direction in which the cutting force is minimized. Consequently, it is necessary to take the partial derivative of Eq. (11):

$$\frac{\partial F}{\partial\alpha} = \frac{ch\cos\varphi\cos(\varphi+\beta+2\alpha+\gamma)}{(b+1)\sin^2\alpha\cos^2(\varphi+\beta+\alpha+\gamma)} \tag{12}$$

By setting Eq. (12) equal to zero, the solution is obtained as follows:

$$\alpha = \frac{\pi}{4} - \frac{\varphi+\beta+\gamma}{2} \tag{13}$$

By substituting Eq. (13) into Eq. (11), F can be determined as follows:

$$F = \frac{2ch\cos\varphi}{(b+1)\,[\sin(\varphi+\beta+\gamma)-1]} \tag{14}$$

Based on the geometric relationships in Fig. 1, F_t in the vertical direction and F_e in the horizontal direction can be computed as follows:

$$\begin{cases} F_t = F\sin(\beta+\gamma) = \frac{2ch\cos\varphi\sin(\beta+\gamma)}{(b+1)[\sin(\varphi+\beta+\gamma)-1]} \\ F_e = F\cos(\beta+\gamma) = \frac{2ch\cos\varphi\cos(\beta+\gamma)}{(b+1)[\sin(\varphi+\beta+\gamma)-1]} \end{cases} \tag{15}$$

The aforementioned solutions pertain to the damage occurring at point O (Fig. 2), where L represents the length of the drill bit's cutting blade composite and n represents the number of composite cutting blades. By integrating F_t and F_e in the direction of the blade, F_T and F_E of the drill bit can be derived as follows:

$$\begin{cases} F_T = \int_0^L F_t dl = \frac{2ch\cos\varphi\sin(\beta+\gamma)nL}{(b+1)[\sin(\varphi+\beta+\gamma)-1]} \\ F_E = \int_0^L F_e dl = \frac{2ch\cos\varphi\cos(\beta+\gamma)nL}{(b+1)[\sin(\varphi+\beta+\gamma)-1]} \end{cases} \tag{16}$$

According to research conducted by Wang Qi et al.[40], the cutting depth of the drill bit can be articulated as follows:

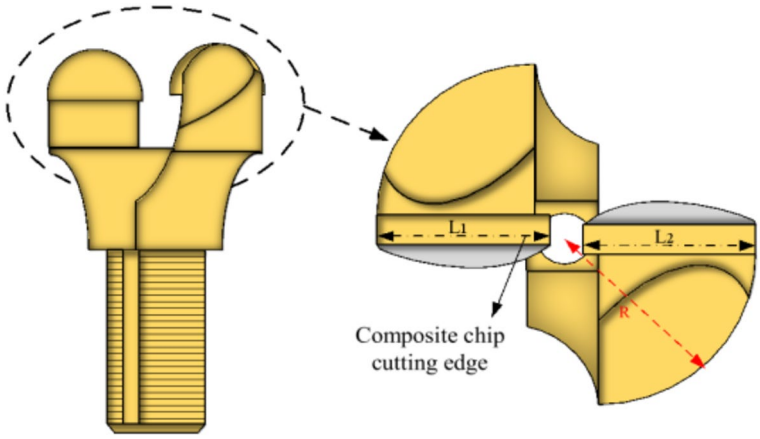

Fig. 2. Schematic of drill bit.

$$h = \frac{v}{nN} \tag{17}$$

where v represents the Rate of Penetration of the drill bit; n represents the number of cutting blade composites; and N represents the rotational speed of the drill bit.

By substituting Eq. (17) into Eqs. (15) and (16), the following results can be obtained:

$$\begin{cases} F = \frac{2cv\cos\varphi}{nN(b+1)[\sin(\varphi+\beta+\gamma)-1]} \\ F_T = \frac{2cv\cos\varphi\sin(\beta+\gamma)L}{N(b+1)[\sin(\varphi+\beta+\gamma)-1]} \\ F_E = \frac{2cv\cos\varphi\cos(\beta+\gamma)L}{N(b+1)[\sin(\varphi+\beta+\gamma)-1]} \end{cases} \tag{18}$$

By integrating F_E in the horizontal direction along the axis of the composite blade, M_E associated with the cutting force can be determined.

$$M_E = \int_{R-L}^{R} nF_E l dl = \frac{cv\cos\varphi\cos(\beta+\gamma)\left(2RL-L^2\right)}{N\left(b+1\right)\left[\sin(\varphi+\beta+\gamma)-1\right]} \tag{19}$$

The aforementioned calculations indicate a specific relationship between cutting force and drilling parameters. When the rotational speed is held constant, both cutting force and torque exhibit an increase as Rate of Penetration rises. Conversely, when Rate of Penetration is maintained at a constant level, an increase in rotational speed results in a decrease in both cutting force and torque.

The specific energy associated with drilling, defined as the energy required to excavate a unit volume of rock, serves as an indicator of the challenges encountered during the drilling process[27]. In accordance with the law of conservation of energy, during rock-breaking operations, the drill bit primarily penetrates the rock mass as a result of the applied drilling force. The rock is fractured through the rotational motion of the drill bit. The work performed W_F by the drilling force in compressing and fracturing the rock, in conjunction with W_M executed by the torque in rotating and shearing the rock W_M, is equivalent to the total energy E_S expended in cutting and breaking the rock, as well as E_T produced during the interaction between the drill bit and the bottom of the borehole.

These variables shows the following relationship:

$$W_F + W_M = E_S + E_T \tag{20}$$

where W_M represents the work performed, during the rock cutting and breaking process with the drill rig applying torque is determined as follows:

$$W_M = 2\pi NMt \tag{21}$$

where N represents the rotational speed of the drill bit; M represents the torque applied by the drill rig; and t represents the drilling time.

W_F during the rock crushing process with the drill rig applying drilling pressure is given as follows:

$$W_F = Fvt \tag{22}$$

where F represents the drilling pressure applied by the drill rig; v represents the Rate of Penetration of the drill bit; and t represents the drilling time.

In Fig. 2, it is assumed that the drill bit utilized for this analysis possesses a radius R, equipped with n diamond composite blades, each of uniform length $L_1 = L_2 = L_3 = \cdots\cdots = L$. During the process of rock crushing under drilling pressure, each diamond composite blade is subjected to an equal normal pressure P :

$$P = \frac{L}{L + L + \cdots + L} F = \frac{1}{n} F \tag{23}$$

Assuming that the coefficient of friction between the diamond composite and the rock at the bottom of the hole is μ , the friction force on each diamond composite piece F_f for:

$$F_f = P\mu \tag{24}$$

Then the frictional moment on each diamond composite piece m_f for:

$$m_f = \left(R - \frac{L}{2}\right) F_f \tag{25}$$

In summary, the frictional force f and E_T generated by the interaction with the rock at the bottom of the hole are expressed as follows:

$$E_T = n \cdot 2\pi N m_f t = 2\pi N \mu F t \left(R - \frac{L}{2}\right) \tag{26}$$

By substituting the aforementioned formulas into Eq. (20), E_S required for the cutting and breaking of rock is derived.

$$E_S = 2\pi NMt - 2\pi RN\mu Ft + \pi N\mu Ft + Fvt \tag{27}$$

The energy necessary to fracture a unit volume of rock during the drilling process is denoted as η_S.

$$\eta_S = \frac{E_S}{V} \tag{28}$$

$$V = \pi R^2 s \tag{29}$$

$$s = vt \tag{30}$$

where V represents the total volume of rock cut and broken and s represents the drilling advance distance.

The solution can be obtained as follows:

$$\eta_S = \frac{2\pi NM - 2\pi RN\mu F + \pi N\mu F + Fv}{\pi R^2 v} \tag{31}$$

The process of drilling and rock fragmentation performed by the drill bit constitutes a coordinated operation involving both the development and rotation systems of the drilling rig. This process is subject to impact from a variety of factors. The research presented in this paper concludes that there exists a mathematical correlation between the energy required to fracture a unit volume of rock using the drill bit and several key parameters: the rotational speed of the drill bit, the torque exerted by the drilling rig, and the Rate of Penetration of the drill bit. Consequently, through the real-time monitoring of these drilling feedback signals (e.g., the drill bit's rotational speed, the torque applied by the drilling rig, and the Rate of Penetration of the drill bit), it is possible to infer the strength of the roof rock and to achieve real-time predictions regarding areas of deterioration within the roof.

Numerical simulation

In order to analyze the relationship between the drilling feedback signals of the drill bit under different conditions, a geometric model of the drill bit and the rock specimen was established using SolidWorks, and the geometric model was assembled and then imported into Abaqus software to establish a simulation model of the interaction between the drill bit and the rock. The geometric model was assembled and imported into Abaqus software to establish the simulation model that A baqus software is a finite element analysis Numerical simulation software which is viewed as is to replace a simpler problem with a complex problems after solving for equilibrium, and viewing the solution domain as is composed of many small elements called finite elements that are small and mutually components of the problem, assume a suitable approximate solution for each unit, and then derive the total satisfaction conditions for solving this domain to obtain a solution to the problem[41–43]. Modeling The rock size is 80 mm × 80 mm × 40 mm and the drill bit size is Φ 30 mm × 50 mm, modeled as shown in Fig. 3. The Drucker-Prager criterion is used for the rock ontological relationship. For this simulation, a two-wing PDC bit (half piece) was used for the rock-breaking drill bit, the simulation builds the drill as shown in Fig. 4, and three different rock materials were used for the drilled rock specimens, namely, yellow sandstone, red sandstone and gray sandstone. The parameters of the three rock materials are shown in Table 1.

In the proposed model, the drill bit and the rock body being drilled are in a state of frictional contact, with the dynamic friction coefficient in the tangential direction set at 0.3. The drill bit is characterized as a rigid body, and its deformation is not considered. To accurately simulate the drilling of an entire roof rock layer, fixed boundary conditions are implemented around the specimen and at its bottom edge (i.e.,

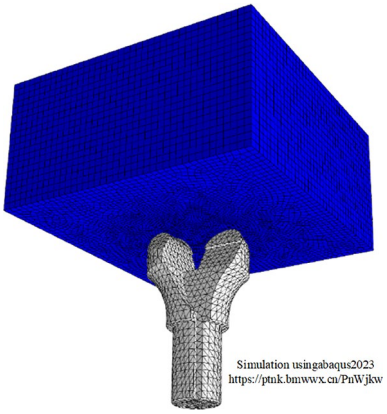

Fig. 3. Schematic of drilling model.

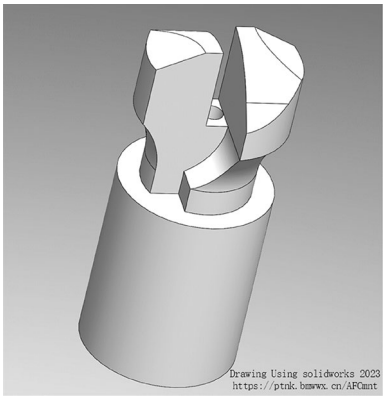

Fig. 4. Schematic of two-wing PDC drill bit.

Type of rock	Elastic modulus ($\times 10^4$ MPa)	Poisson's ratio	Compressive strength (MPa)	Tensile strength (MPa)	Shear strength (MPa)	Internal friction angle
Yellow sandstone	1.33	0.15	42.87	2.33	8.63	31.1
Red sandstone	2.35	0.19	62.51	4.67	11.74	32.53
Grey sandstone	5.25	0.22	102.54	5.73	19.61	35.37

Table 1. Mechanical and physical properties of rock materials.

$U_x = U_y = U_z = UR_x = UR_y = UR_z = 0$), thereby ensuring the stability of the rock specimen. For the purpose of simplifying the drilling process, the drill bit is permitted to rotate and move along the Y-axis, while vibrations in the X and Z directions are disregarded. In order to approximate the rate of penetrations during drilling in real coal mines, the rate of penetrations in the numerical simulation were set to 20 mm/s, 25 mm/s, and 30 mm/s respectively. This simulation encompasses three scenarios for analysis, each with specific parameter settings as detailed below:

(1) The Rate of Penetrations should be set at 20 mm/s, 25 mm/s, and 30 mm/s, while maintaining a constant rotational speed of 500 r/min for the simulation of drilling in grey sandstone.
(2) The rotational speeds were set at 300 r/min, 400 r/min, and 500 r/min, while maintaining a constant Rate of Penetration of 30 millimeters per second (mm/s) for the simulation of drilling in grey sandstone.
(3) A constant Rate of Penetration of 30 mm/s and a constant rotational speed of 500 r/min should be established, followed by conducting drilling simulations on yellow sandstone, red sandstone, and grey sandstone.

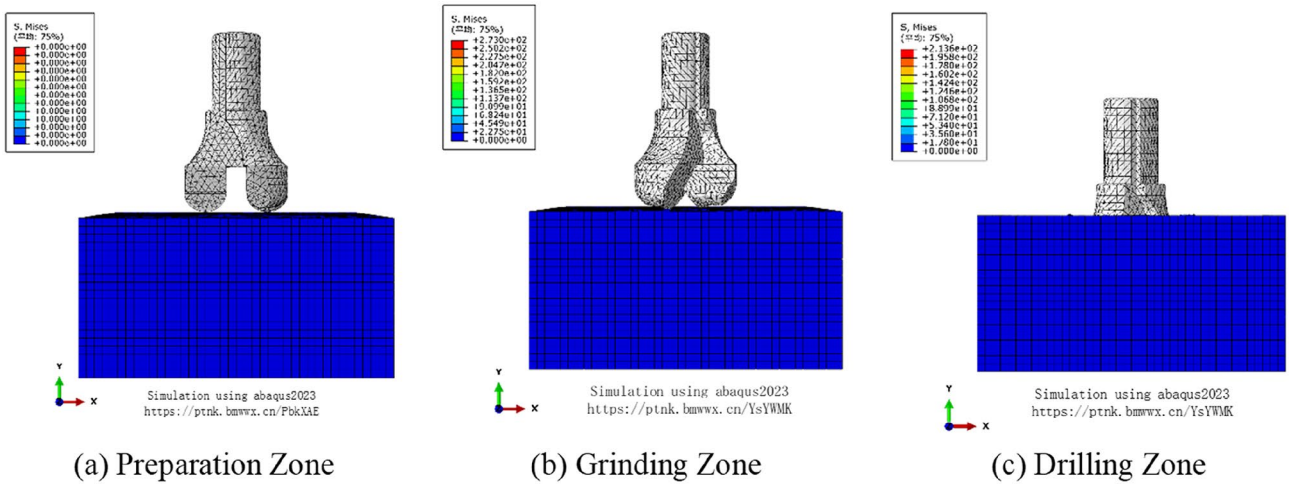

Fig. 5. Schematic of drilling process.

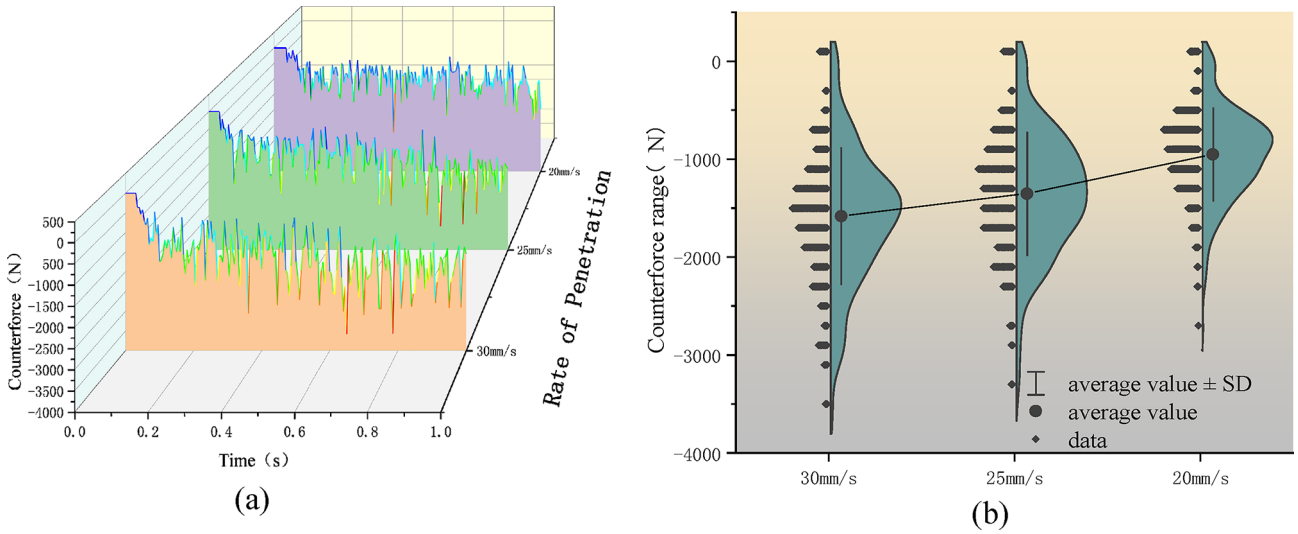

Fig. 6. Numerical simulation of reaction forces on drill bit at different rate of penetrations.

Analysis of numerical simulation

Drilling process

The drilling process can be categorized into four stages based on the relative positioning of the drill bit and the rock: the preparation zone, grinding zone, drilling zone, and completion zone. In the preparation zone, the drill bit has yet to make contact with the rock specimen, resulting in no alterations to the stress components. During the grinding zone, the thrust exerted by the drill rod enables the cutting blade of the drill bit to penetrate the rock specimen. As the cutting blade continues its upward trajectory, the drill bit engages in cutting the rock specimen under the impact of torque, which is referred to as the drilling zone. This stage is characterized by the formation of a stable drilling channel within the rock specimen, persisting until the drill bit has fully penetrated the rock, thereby entering the completion zone (Fig. 5). In practical drilling operations, the occurrence of blockages may necessitate the identification of an additional stage within the drilling zone, termed the blockage zone. The numerical simulation conducted in this study focused exclusively on the drilling zone and did not explore the other stages. The results of the numerical simulation indicate that the reaction force acting on the drill bit and the cutting force exerted by the drill bit are interrelated action and reaction forces.

Drilling simulations at different rate of penetrations

To investigate the feedback signals of the drill bit at varying Rate of Penetrations, the simulation setup applies a rotational speed of 500 r/min in the positive Y direction, while Rate of Penetrations of 20 mm/s, 25 mm/s, and 30 mm/s are imposed in the negative Y-axis direction. The computed results for the reaction force and reaction torque acting on the drill bit are illustrated in Figs. 6 and 7.

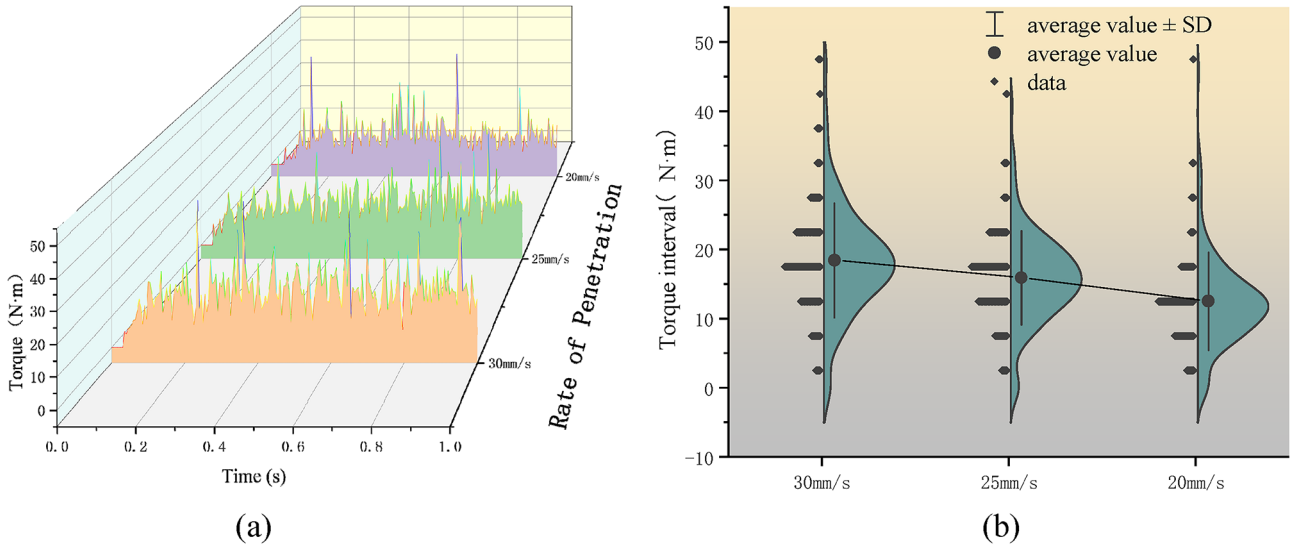

Fig. 7. Numerical simulation of reaction torques on drill bit at different rate of penetrations.

The analysis of Figs. 6 and 7 reveals that the reaction force exerted on the drill bit exhibits periodic oscillations. This phenomenon can be attributed to the rock specimen utilized in the simulation software, which is constructed from numerous uniform grids. Upon the cutting of the rock, these grids fracture and shift, resulting in fluctuations within the simulation results that manifest as periodic variations. In real-world production scenarios, as the drill bit penetrates a homogeneous rock body, the feedback signals generated during the drilling process similarly display periodic oscillatory changes.

It indicates that the Rate of Penetration significantly impacts the reaction force experienced by the drill bit. When maintaining a constant rotational speed, an increase in Rate of Penetration results in a greater volume of rock being cut per unit of time, as well as an increase in the energy required to fracture a unit volume of rock. Consequently, this leads to an increase in both the thrust and torque experienced by the drill bit. Figures 6b and 7b demonstrate that, throughout the drilling process, the average cutting force and torque exhibit an upward trend in relation to Rate of Penetration. In other words, when drilling through a uniform rock formation, the average values of cutting force and torque are positively correlated with the Rate of Penetration. Although variations in Rate of Penetration impact the distribution thresholds of cutting force and torque, these thresholds do not exhibit a clear correlation with other influencing factors.

Drilling simulations at different rotational speeds

To analyze the drilling feedback signals at varying rotational speeds, the simulation setup employs a Rate of Penetration of 30 mm/s directed along the negative Y-axis for PDC drill bit. Additionally, three rotational speeds of 300 r/min, 400 r/min, and 500 r/min are established for the simulation trials. The computed results pertaining to the reaction force and reaction torque experienced by the drill bit are depicted in Figs. 8 and 9.

The data in Figs. 8 and 9 indicate that rotational speed significantly impacts the cutting force during the drilling process. Specifically, an increase in rotational speed is associated with a reduction in torque (Figs. 8b and 9b). It indicates that the average values of both reaction force and reaction torque diminish as rotational speed increases. Consequently, when drilling through a uniform rock body at a constant Rate of Penetration, both the cutting force and torque of the drill bit exhibit a decreasing trend with rising rotational speed, thereby establishing a negative correlation between the drill bit's rotational speed and its cutting force and torque.

As the rotational speed increases (Fig. 8b), the average reaction force exerted on the drill bit exhibits a decreasing trend, accompanied by a reduction in the oscillation threshold of the reaction force. Conversely, in Fig. 9b, while the reaction torque similarly demonstrates a decreasing trend with increasing rotational speed, the oscillation threshold of the reaction torque does not exhibit a discernible change. This observation suggests that rotational speed does not significantly impact the oscillation threshold of the reaction torque.

Drilling simulations on different rock types

This simulation setup involved the selection of three rock types (e.g., yellow sandstone, red sandstone, and grey sandstone) as the models for the three simulation trials. The parameters of the models are detailed in Table 1. A Rate of Penetration of 30 mm/s in the negative Y direction and a rotational speed of 500 r/min were applied to PDC drill bit. The calculated results for the reaction force and reaction torque acting on the drill bit are presented in Figs. 10 and 11.

The materials utilized in this numerical simulation indicate that grey sandstone exhibits the highest compressive strength, followed by red sandstone, while yellow sandstone demonstrates the lowest compressive strength. In Figs. 10 and 11, the strength of the rock significantly impacts the cutting force and torque during the drilling process. Specifically, the cutting force and torque are maximized when drilling into grey sandstone and

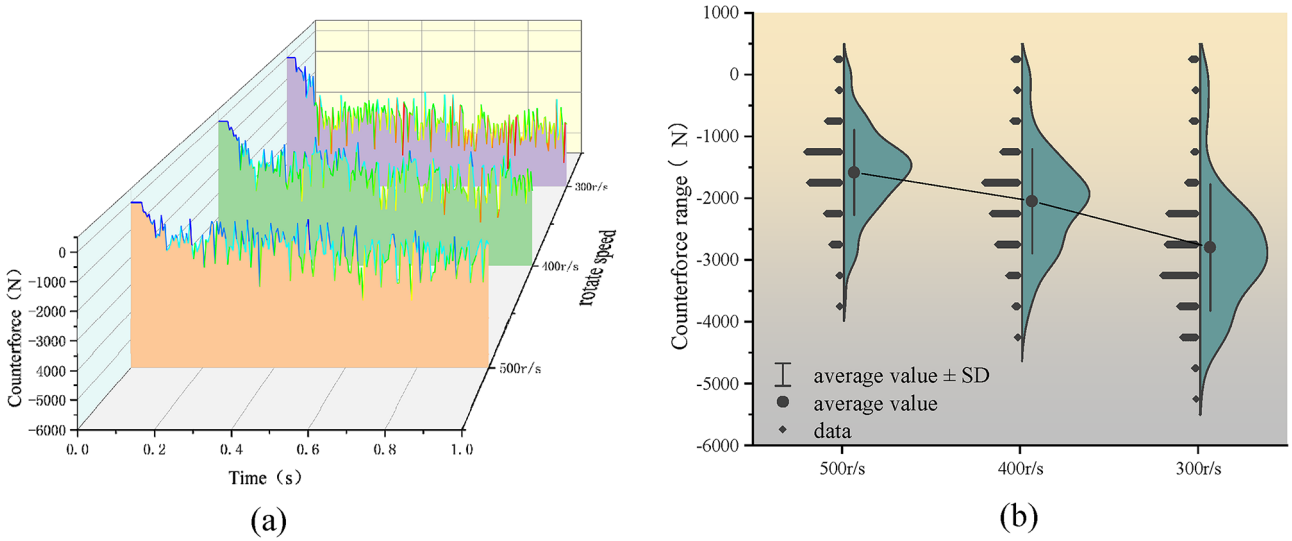

Fig. 8. Numerical simulation of reaction forces on drill bit at different rotational speeds.

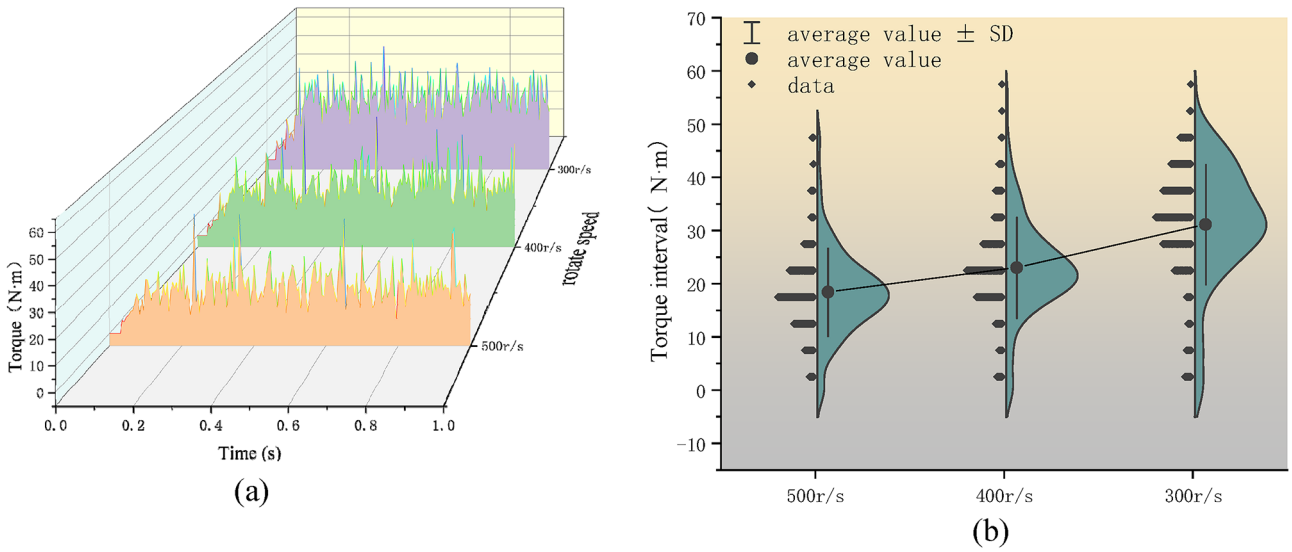

Fig. 9. Numerical simulation of reaction torques on drill bit at different rotational speeds.

minimized when drilling into yellow sandstone. Consequently, under conditions of constant Rate of Penetration and rotational speed, both the cutting force and torque of the drill bit increase in correlation with the strength of the rock.

In Figs. 10a and 11a, the oscillation thresholds of the reaction force and reaction torque diminish as the uniaxial compressive strength of the rock materials decreases. Furthermore, Figs. 10b and 11b illustrate that the data distribution thresholds for the reaction forces and torques are widest for grey sandstone and narrowest for yellow sandstone. Although the strength difference between yellow sandstone and red sandstone is minimal, the average values of the cutting force and torque do not exhibit significant variation. However, the oscillation thresholds (data distribution thresholds) of the reaction forces and torques can effectively highlight the differences in rock strength. Consequently, it can be inferred that the oscillation thresholds of the cutting force and torque in the drilling feedback signals may also serve as indicators for deducing the compressive strength of the drilled rock layers.

Self-research drilling experiments

To further substantiate the reasoning presented previously, this study developed a drilling experiment platform that is capable of real-time collection of drilling parameters. This platform is designed to accommodate various parameter sensors, enabling the execution of drilling experiments on different rock specimens. Figure 12 depicts a schematic of the experimental setup. The structure of the experimental platform primarily comprises

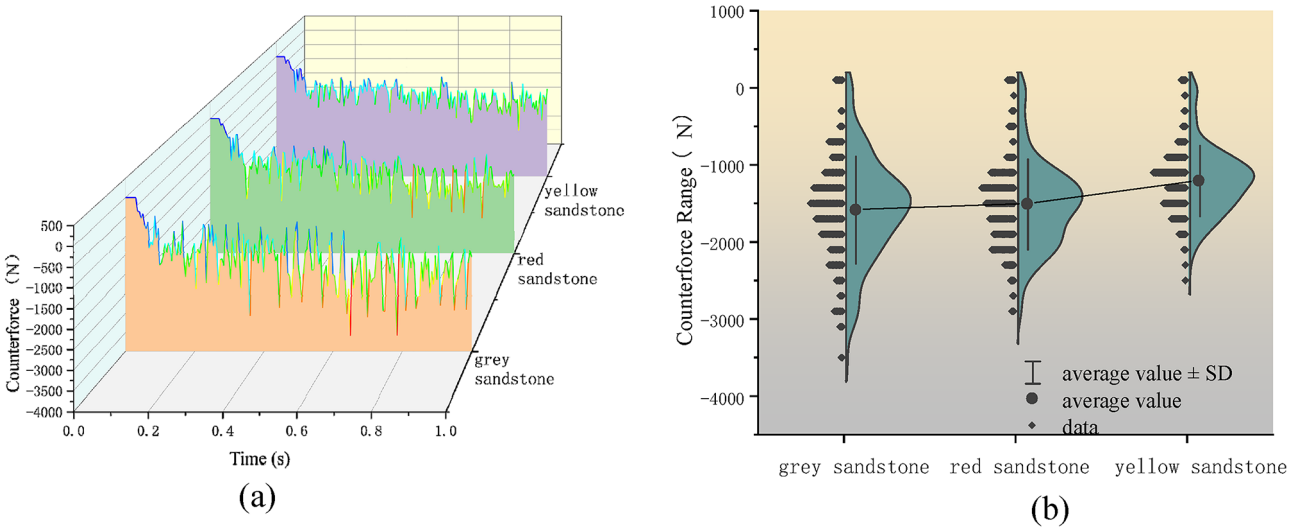

Fig. 10. Numerical simulation of reaction forces on drill bit across different rock types.

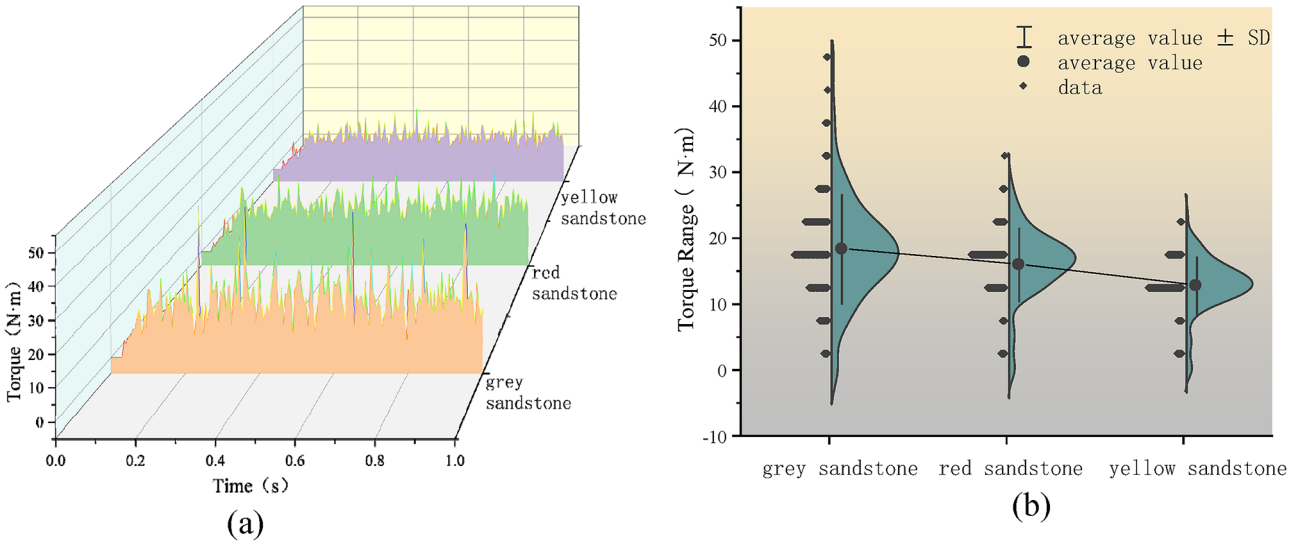

Fig. 11. Numerical simulation of reaction torques on drill bit across different rock types.

a hydraulic lift, a specimen preparation platform, a crawler-type anchor drilling rig, and a drilling information collection system.

To compare the results obtained from numerical simulations, the selected test specimens consist of yellow sandstone, red sandstone, white sandstone, and grey sandstone, each with dimensions of 180 mm × 180 mm × 300 mm. The fundamental mechanical parameters of these four types of prefabricated rock specimens are presented in Table 1. A two-wing PDC drill bit, with a diameter of 32 mm, is utilized in conjunction with a B19-type drill rod measuring 1.2 m in length for the drilling operations. The Rate of Penetration and rotational speed are initially regulated by the hydraulic system of the drilling rig, achieving a no-load Rate of Penetration of 30 mm/s and a rotational speed of 500 r/min. During the drilling process, various parameters, including displacement, thrust, rotational speed, and torque, are recorded.

The drilling process of rocks has been previously analyzed (Fig. 13). The stage characterized by the absence of displacement change is identified as the preparation zone. The initial contact point of the drill bit with the rock specimen signifies the commencement of the grinding zone. The subsequent occurrence of displacement changes, culminating in peak displacement, delineates the drilling zone stage. At the onset of this stage, both thrust and torque experience a marked increase. The transition to a phase of periodic oscillations in thrust and torque indicates the establishment of a stable drilling stage. As thrust and torque subsequently decline and displacement begins to decrease, the drilling phase concludes; at this point, a complete drill hole has been formed, penetrating the rock and initiating the withdrawal operation, which is referred to as the completion zone. Within the completion zone, both thrust and torque decrease from their maximum values to their minimum levels.

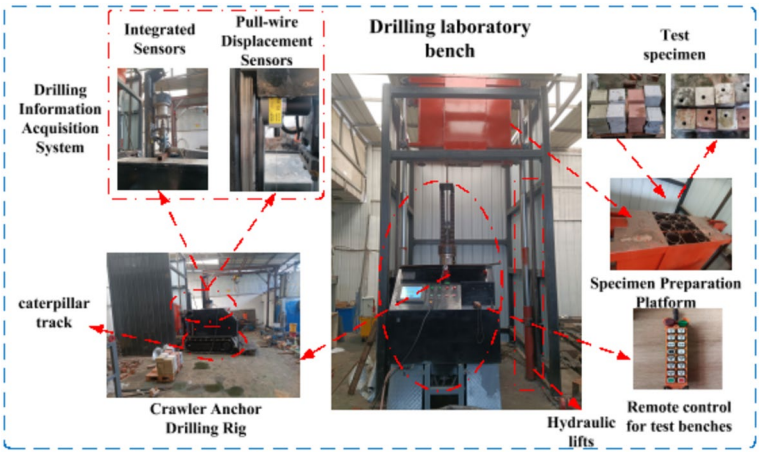

Fig. 12. Schematic of drilling equipment setup.

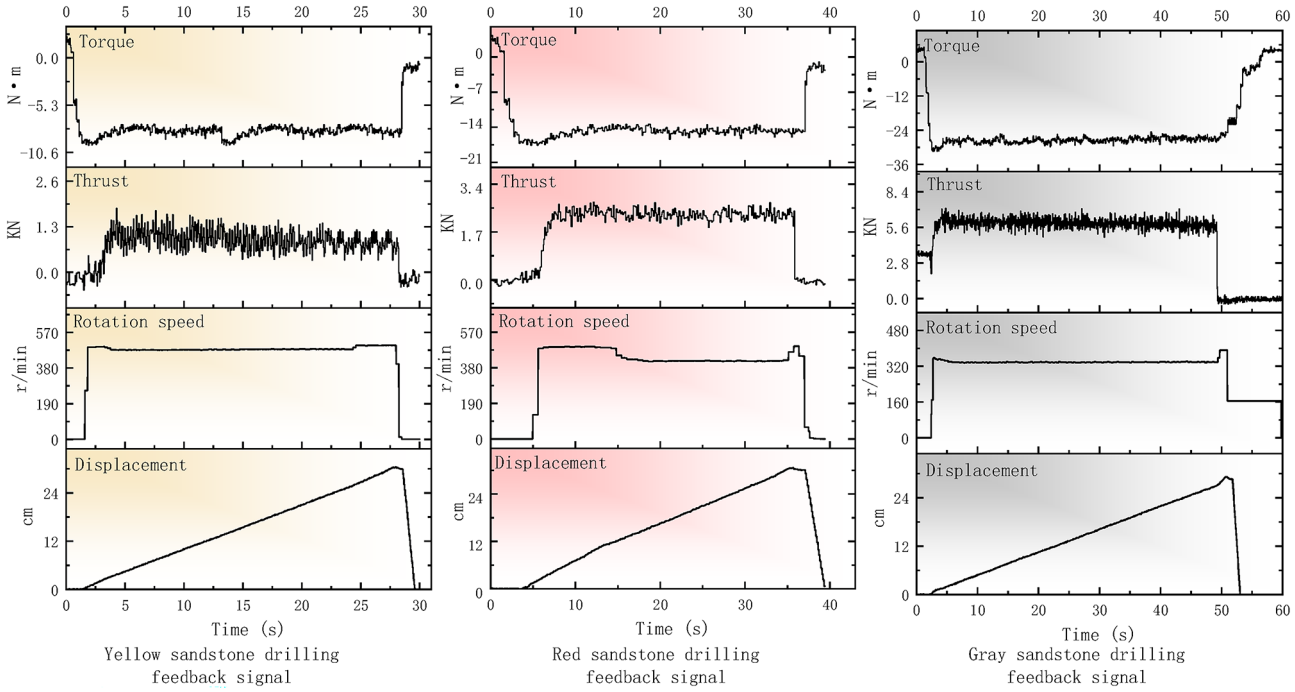

Fig. 13. Line chart of drilling feedback signals across different rock types.

This data originates from one of four experimental groups that completed the drilling construction. The remaining three groups encountered operational errors, including jamming and deviation, during the testing process, which prevented them from completing the construction of the drill hole. While this process reflects the blockage zone encountered in actual drilling operations, the data pertaining to this zone is incomplete and does not facilitate a systematic comparative analysis; consequently, this phase is not addressed in this study. The variations in data at different time points, as depicted in the diagram, effectively illustrate the preparation zone, grinding zone, drilling zone, and completion zone throughout the drilling process. Upon initially entering the stable drilling stage, the drill bit makes contact with the rock specimen but has not yet established a stable drilling channel, resulting in significant fluctuations in thrust and torque values. Once the drill bit reaches a sufficient depth to create a stable channel, the fluctuations in drilling parameters are significantly reduced.

In the analysis of the rotational speed and Rate of Penetration of the drill bit during the stable drilling phase across various rock strengths, the drill bit achieves its maximum rotational and Rate of Penetrations when penetrating yellow sandstone, while it exhibits the minimum rotational and Rate of Penetrations when engaging with grey sandstone. Operational errors associated with the drilling rig have led to inadequate control of the drill bit's rotational speed in both the grinding and completion zones, resulting in abnormal fluctuations in rotational speed. Furthermore, an examination of the thrust exerted during the stable drilling phase across different rock

strengths reveals that the drill bit applies the least thrust when drilling into yellow sandstone and the most thrust when drilling into grey sandstone. This observation suggests that the average thrust during the drilling process increases in correlation with the strength of the rock. Additionally, an assessment of the torque during the stable drilling phase indicates that the torque is at its lowest when drilling into yellow sandstone and at its highest when drilling into grey sandstone. This result further supports the conclusion that the average torque during the drilling process also increases with the strength of the rock.

Discussion

Both numerical simulations and theoretical analyses have demonstrated that an increase in rock strength correlates with a decrease in both the average Rate of Penetration and the rotational speed of the drill bit, while thrust and torque exhibit an increase. Specifically, the average Rate of Penetration and rotational speed of the drill bit are negatively correlated with rock strength, whereas thrust and torque are positively correlated. This conclusion aligns with experimental results, and the accuracy of these results has been mutually validated. Consequently, it is feasible to predict rock strength based on drilling feedback signals observed during the stable drilling phase. It is posited that abrupt changes in drilling feedback signals during the construction of anchor holes in tunnels can accurately reflect sudden alterations in the structural integrity of the roof rock layers. Furthermore, building upon the aforementioned research, it is possible to infer trends regarding the changes in the surrounding rock structure of tunnel roofs.

Although there is a large body of research on structural probing of rock formations with drilling. Reference[44] takes into account that the action of the rock body on the drill bit generates a feedback signal that is related to the formation seam, etc.; literature[45] considering the interrelationship between the drill bit Interrelationship between force and vibration acceleration Study of different lithological differentiation.; literature[46] considered the correlation between drilling parameters and top plate interrelationships between the void structure to make a structural determination of the formation; All of these studies have provided a basis for structural detection with drilling a basis for structural detection with drilling, but each method has its shortcomings. Literature[44] analyzed from the experimental point of view missing the validation of numerical simulations, literature[45] no experiments were set up to validate and analyze the simulation results that Literature[46] only considering the roof void structure The lithology was not explored. In contrast, this study analyzes the mechanism of drilling rock breaking, establishes a numerical simulation model, and independently develops a laboratory drilling experimental platform for validation, and analyzes the interrelationships between drilling feedback signals and lithology from the perspective of combining experiments and numerical simulations.

Conclusion

This study provides a comprehensive investigation into the mechanisms of drilling and rock-breaking, establishing critical functional relationships between the cutting forces exerted by drill bits and the energy required to break a unit volume of rock. Through simulations utilizing Abaqus finite element software, this study explored the interactions between drilling feedback signals and various rock types and drilling parameters. A custom-designed drilling experiment platform was developed for real-time collection of key drilling parameters, including displacement, rotational speed, thrust, and torque. Experimental results from three types of prefabricated rocks were compared against theoretical models and numerical simulations, yielding the following conclusions:

1. During the drilling process, rock-breaking is primarily achieved through the vertical thrust of the drill rod advancing the drill bit and the torque applied in the horizontal direction rotating the bit. Assuming that the cutting force on the fractured rock surface follows a power function distribution, this study developed functional relationships for the cutting force F and torque M_E of the drill bit. Additionally, a functional relationship for the energy η_S required to break a unit volume of rock was derived. The study determined that with constant rotational speed, cutting force and torque increase with Rate of Penetration. Conversely, with constant Rate of Penetration, cutting force and torque decrease as rotational speed increases
2. (2) The entire process of the drill bit cutting through rock was simulated using Abaqus software, analyzing results across different Rate of Penetrations, rotational speeds, and rock types. Based on the relative position of the drill bit and rock, the drilling process was divided into four phases: preparation zone, grinding zone, drilling zone, and completion zone. In the stable drilling phase (drilling zone), reaction forces and torques increased with increasing Rate of Penetration and decreased with increasing rotational speed. Higher rock strength resulted in greater reaction forces and torques experienced by the drill bit.
3. A drilling experiment platform capable of real-time collection of drilling parameters was developed, accommodating various parameter sensors to conduct experiments on rock specimens with different properties. Experiments conducted on three types of prefabricated rocks revealed that as rock strength increases, both the rotational speed and Rate of Penetration decrease, while thrust and torque increase. This highlights the need to adjust drilling parameters based on rock strength for optimal performance.
4. Comparative analyses of the relationships between rock strength and drilling feedback signals, derived from theoretical deductions, numerical simulations, and experimental results, demonstrated consistent results. As rock strength increases, the average Rate of Penetration and rotational speed decrease, while thrust and torque increase. This establishes a negative correlation between rock strength and both Rate of Penetration and rotational speed, and a positive correlation between rock strength and thrust and torque. These conclusions were validated across all three approaches. Furthermore, during the construction of anchor holes in tunnels, sudden changes in drilling feedback signals can provide reliable indicators of structural changes in the surrounding rock layers. By analyzing the relationship between the surrounding rock structure and feedback signals, it can predict trends in the roof rock structure changes.

Data availability

The raw data supporting the conclusion of this article will be made available by the authors, without undue reservation. Xiao-He Wang (wangxh_1994@163.com) should be contacted if someone wants to request the data from this study.

Received: 18 December 2024; Accepted: 18 April 2025
Published online: 25 April 2025

References

1. Yuan, L. Strategic conception of carbon neutralization in coal industry. *Strategic Study CAE*. **25**(5), 103–110 (2023).
2. Wang, G. et al. Development and innovation practice of China coal mining technology and equipment for 50 years: commemorate the 50th anniversary of the publication of coal science and technology. *Coal Sci. Technol.* **51**(1), 1–18 (2023).
3. Guo, S. Recognizing method of coal roadway roof strata based on the vibration characteristics of bolter. Doctoral Dissertation. In *China University of Mining and Technology (Beijing)* (2018, accessed 23 Sep 2024).
4. Qiao, B. Research on rock identification and drilling response mechanism in potential falling zone of roadway roof. Doctoral Dissertation. In *China University of Mining and Technology (Beijing)* (2023).
5. Evans, I. The force required to cut coal with blunt wedges. *Int. J. Rock. Mech. Min. Sci. Geomech. Abstracts* **2**(1), 1–12 (1965).
6. Evans, I. A theory of the cutting force for point-attack picks. *Int. J. Min. Eng.* **2**(1), 63–71 (1984).
7. Evans, I. A theory of the basic mechanics of coal ploughing. *Min. Res.* **1962**, 761–798 (1962).
8. Nishimatsu, Y. The mechanics of rock cutting. *Int. J. Rock. Mech. Min. Sci. Geomech. Abstracts*. **9**(2), 261–270 (1972).
9. Goktan, R. M. & Gunes, N. A semi-empirical approach to cutting force prediction for point-attach picks. *J. South Afr. Inst. Min. Metall.* **105**(4), 257–263 (2005).
10. Roxborough, F. F. & Liu, Z. C. Theoretical considerations on pick shape in rock and coal cutting (1995).
11. Yasar, S. A. General Semi-Theoretical model for conical picks. *Rock. Mech. Rock. Eng.* **53**(6), 2557–2579 (2020).
12. Bilgin, N. et al. Dominant rock properties affecting the performance of conical picks and the comparison of some experimental and theoretical results. *Int. J. Rock. Mech. Min. Sci.* **43**(1), 139–156 (2006).
13. Cheng, Z. et al. Imaging the formation process of cuttings: characteristics of cuttings and mechanical specific energy in single PDC cutter tests. *J. Petrol. Sci. Eng.* **171**, 854–862 (2018).
14. Wang, X., Wang, Z., Wang, D. & Chai, L. A novel method for measuring and analyzing the interaction between drill bit and rock. *Measurement* **121**, 344–354. https://doi.org/10.1016/j.measurement.2018.02.045 (2018).
15. Liu, W., Zhu, X. & Li, B. The rock breaking mechanism analysis of rotary percussive cutting by single PDC cutter. *Arab. J. Geosci.* **11**(9), 192 (2018).
16. Saksala, T. Numerical study of the influence of hydrostatic and confining pressure on percussive drilling of hard rock. *Comput. Geotech.* **76**, 120–128 (2016).
17. Zhu, X., Liu, W. & He, X. Numerical simulation analysis of rock cutting based on discrete element method. *J. Basic. Sci. Eng.* **25**(3), 509–520. https://doi.org/10.16058/j.issn.1005-0930.2017.03.008 (2017).
18. Zhang, Y., Zhang, N., Liu, P., Ju, P. & He, Y. Study on drilling dynamic characteristics and formation information identification of anchorage hole in typical coal-bearing strata. *Coal Sci. Technol.* **49**(2), 177–185 (2021).
19. Liu, S., Liu, D., Feng, Y., Li, X. & Shang, P. Influence of stress state on rate of penetration of roof anchoring hole in coal roadway. *J. China Coal Soc.* **39**(4), 608–613 (2014).
20. Fu, M., Liu, S. & Jia, H. Study on the influence of dynamic parameters of bolter on the drilling characteristics of roof anchoring hole in coal roadway. *J. Min. Saf. Eng.* **35**(3), 517–524 (2018).
21. Meng, X. et al. Numerical simulation study on vibration characteristics of Drill pipe drilling in anchor hole of roof in coal roadway. *J. Min. Saf. Eng.* **36**(3), 473–481 (2019).
22. Han, R. Vibration measurement while drilling method of mine drilling rig and its application. Master Thesis. In *China University of Mining and Technology* (2017, accessed 23 Sep 2024).
23. Niu, G. Theory and application of rock mass quality evaluation based on response characteristics of drilling rig. Doctoral Dissertation. *China University of Mining and Technology* (2023).
24. Liu, Y. et al. Research on rock strength identification while drilling based on impact rotary drilling. *Rock. Soil. Mech.* **45**(3), 857–866 (2024).
25. Wang, S., Wu, Y., Cai, X. & Zhou, Z. Rock strength prediction and drillability identification based on drilling parameters. *J. Cent. South. Univ.* **30**(12), 4036–4051 (2023).
26. Wang, Y., Yu, Q., Niu, P. & Li, Y. Research on characterization model of rock uniaxial compressive strength based on drilling parameters. *J. Northeastern Univ. (Nat. Sci.)* **44**(8), 1168–1176 (2023).
27. Wang, Q. et al. Relationship between drilling parameters of digital drilling and uniaxial compressive strength of rock. *J. China Coal Soc.* **43**(5), 1289–1295 (2018).
28. Rodgers, M. et al. Measuring rock strength while drilling shafts socketed into Florida limestone. *J. Geotech. GeoEnviron. Eng.* **144**(3), 04017121 (2018).
29. Yaşar, E., Ranjith, P. G. & Viete, D. R. An experimental investigation into the drilling and physico-mechanical properties of a rock-like brittle material. *J. Petrol. Sci. Eng.* **76**(3), 185–193 (2011).
30. Shreedharan, S., Hegde, C., Sharma, S. & Vardhan, H. Acoustic fingerprinting for rock identification during drilling. *Int. J. Min. Mineral. Eng.* **5**(2), 89–105 (2014).
31. Kumar, B. R., Vardhan, H. & Govindaraj, M. Estimating rock properties using sound level during drilling: field investigation. *IJMME* **2**(3), 169 (2010).
32. Kumar, V., Vardhan, H. & Murthy, C. S. N. Multiple regression model for prediction of rock properties using acoustic frequency during core drilling operations. *Geomech. Geoeng.* **15**(4), 297–312 (2020).
33. Vardhan, H. & Suryanarayana Chivukula, M. An experimental investigation of Jack hammer drill noise with special emphasis on drilling in rocks of different compressive strengths. *Noise Control Eng. J.* **55**, 56 (2007).
34. Vardhan, H., Adhikari, G. R. & Govinda Raj, M. Estimating rock properties using sound levels produced during drilling. *Int. J. Rock Mech. Min. Sci.* **46**(3), 604–612 (2009).
35. Hoffman, M. P. Computer-based monitoring and control of a mast-type roof drill. In *Preprints-Society Of Mining Engineers Of AIME* (1994).
36. Itakura, K. et al. *Development of a Roof Logging System by Rock Bolt Drilling* (Coal and Safety, 1997).
37. Itakura, K. Current drill monitoring system using mechanical data of drilling machine and Estimation of roof rock structure. In *Proceedings of the Aust.-Japan Tech. Exchange Workshop in Coal Mining, vol. 98* 8–10 (1998).
38. ichi Itakura, K., Sato, K., Deguchi, G., Icihara, Y. & Matsumoto, H. Visualization of geostructure by mechanical data logging of rockbolt drilling and its accuracy. In *20th International Conference on Ground Control in Mining* 184–190 (2001).
39. Itakura, K. et al. Portable intelligent drilling machine for visualizing roof-rock geostructure. In *Proceedings of Aachen international mining symposium, Aachen* 597–609 (2008).

40. Wang, Q., Qin, Q., Gao, H., Jiang, B. & Xu, S. Test method of rock c-φ parameters based on digital drilling. *J. China Coal Soc.* **44**(3), 916–923 (2019).
41. Sanei, M. Numerical and experimental study of coupled nonlinear geomechanics and fluid flow applied to reservoir simulation = estudo numérico e experimental de geomecânica não-linear Acoplada a Escoamento de Fluido Em reservatórios (2020).
42. Duran, O. et al. An enhanced sequential fully implicit scheme for reservoir geomechanics. *Comput. Geosci.* **24**, 1557–1587 (2020).
43. Heydari, M., Emamqeysi, A., Sanei, M. & M. R., and Finite element analysis of wellbore stability and optimum drilling direction and applying NYZA method for a safe mud weight window. *J. Anal. Numer. Methods Min. Eng.* **11**(29), 67–76 (2022).
44. Rostami, J. et al. Rock characterization while drilling and application of roof bolter drilling data for evaluation of ground conditions. *J. Rock Mech. Geotech. Eng.* **7**(3), 273–281 (2015).
45. Mengxiong, F. U. et al. Numerical simulation study on the vibration characteristics of drill pipe for drilling of anchor holes in coal mine roof. *J. Min. Saf. Eng.* **36**(03), 473–481 (2019).
46. Finfinger, G. L. *A Methodology for Determining the Character of Mine Roof Rocks* (West Virginia University, 2003).

Author contributions

In this paper, Xiao-He Wang, Wu Jing conducted experiments and collected experimental data; the full text was co-authored by Xiao-He Wang and Zhi-Qiang Zhao. Xiao-He Wang and Wu Jing are responsible for the data analysis and graphics rendering. Xiao-He Wang and Wu Jing are responsible for the data analysis and graphics drawing; Xiao-He Wang, Zhi-Qiang Zhao, and Wu Jing are responsible for the editing of the article.

Funding

This research was funded by National Natural Science Foundation of China (U22A20165)and the Guizhou Province Science and Technology Support Plan Project of China (Qiankehe Support [2021] General 400). This support is gratefully acknowledged. The authors are grateful to the reviewers for discerning comments on this paper.

Competing interests

The authors declare no competing interests.

Additional information

Correspondence and requests for materials should be addressed to Z.-Q.Z.